14 日にはジストロフィンが発現が確認された。MyoD によってマウス胎児由来線維芽細胞が in vitro では筋細胞に分化することが確認された。

MyoD 導入 GFP-MEF 細胞の筋線維への *in vivo* 分化

MyoD 導入 GFP-MEF 細胞を野生型マウス前脛骨筋に移植し 4 週間後に解析した。約 80%の筋線維は GFP 陽性であり、このうち再生線維を中心に GFP 強陽性線維が認められた。MyoD 導入によって線維芽細胞が筋線維に分化し筋再生に参加することが *in vivo* で明らかとなった。これらの GFP 陽性線維のうち、弱陽性線維は内因性筋線維への MyoD 導入 GFP-MEF 細胞の融合、強陽性線維は MyoD 導入 GFP-MEF 細胞からの筋線維の分化が予想される。今後は雄 GFP-MEF 細胞から雌野生型マウスへの細移植をおこない、Y 染色体染色による筋核の同定による検討を予定している。

D. 考察と今後の課題

4 種類の遺伝子発現によって線維芽細胞が胚性多能性幹（iPS 細胞）になるという山中らの報告によって成熟体細胞から多能性幹細胞への“初期化”が証明され、再生療法は新たな時代を迎えている。MyoD は骨格筋分化への最も重要な転写因子と考えられ藤井らはヒト皮膚生検組織からの線維芽細胞へのこの転写因子導入によって *in vitro* では骨格筋への分化に成功した。今回の検討により MyoD を導入したマウス胎児線維芽細胞も *in vitro* で骨格筋へ分化し、更にこの細胞の移植によって *in vivo* でも筋線維に高率に分化することを示した。本研究では MyoD 導入に際してアデノウイルスベクターを用いたが、MyoD の発現は一過性であり宿主ゲノムへのウイルスインテグレイションはないものと考えられた。しかしながらこの細胞移植戦略を FCMD 患者への臨床応用を考えた場合には、ウイルスベクターの使用が安全性、倫理性において問題となると予想される。従って今後は MyoD 導入についてアデノウイルスベクター以外のアプローチについての検討が必要と考えられる。また MyoD 導入マウス胎児線維芽細胞の分化過程での α-DG の糖鎖修飾についての詳細な検討が必須となる。

E.結論

マウス胎生線維芽細胞に骨格筋特異的転写因子である MyoD をアデノウイルスベクターによって導入すると *in vitro* でも *in vivo* でも筋細胞に分化することが明らかとなった。この細胞を用いた FCMD 患者への再生治療法を目指し FCMD モデルマウスへの治療研究を行う予定である。

F.健康危険情報

該当なし

G.研究発表

1. 論文発表

Ohsawa Y, Okada T, Kuga A, Hayashi S, Murakami T, Tsuchida K, Noji S, Sunada Y. Caveolin-3 regulates myostatin signaling. Mini-review.
Acta Myol. 2008 Jul;27:19-24.

2. 学会発表

1)Ohsawa Y, Okada T, Kuga A, Hayashi S, Murakami T, Sunada Y. A small-molecule inhibitor targeting transforming growth factor-b type receptor kinase ameliorate muscular atrophy in a mouse model of caveolin-3-deficient muscular dystrophy. 13th International Congress of World Muscle Society, Newcastle, UK, September 29-October 2(2008)

2) 久我敦、大澤裕、林紗織、村上龍文、砂田芳秀．cardiotoxin 筋再生モデルにおける caveolin-3 と dysferlin の動態. 第 49 回日本神経学会総会、横浜、2008 年 5 月 15 日

3)大澤裕、岡田只士、林紗織、久我敦、村上龍文、若山吉弘、澁谷誠二、砂田芳秀．caveolin-3 欠損筋の dysferlin/myoferlin 細胞内局在異常. 第 49 回日本神経学会総会、2008 年 5 月 15 日

H.知的財産権の出願・登録状況

（予定を含む。）

1. 特許取得
   なし
2. 実用新案登録
   なし
3. その他

厚生労働科学研究費補助金（こころの健康科学研究事業）
分担研究報告書

「POMGnT1欠損マウスを用いたα-dystroglycanの中枢神経系及び骨格筋での機能解析、及びAAV遺伝子治療」

分担研究者　鈴木 友子
国立精神・神経センター神経研究所
遺伝子疾患治療研究部　室長

研究要旨

α-dystroglycan (α-DG)は、骨格筋膜上のジストロフィン・糖蛋白質複合体の主要な構成成分であり、*O*-マンノース型糖鎖を介して細胞外のラミニン、アグリン、パールカン等と結合している。POMGnT1はマンノースにGlcNacを転移する酵素であり、その活性低下により、先天性筋ジストロフィーの一つmuscle-eye-brain病(MEB)が発症する。我々はPOMGnT1変異マウスをgene targeting法を用いて作出し、その筋衛星細胞の増殖能、分化能を調べた。*POMGnT1*$^{-/-}$ではα-DGの糖鎖修飾が異常であったが、組織切片上では骨格筋の筋変性･壊死の程度は軽微であった。POMGnT1$^{-/-}$筋衛星細胞の細胞増殖能は低下していた。α-DG-ラミニンの結合は筋衛星細胞の増殖能の維持に重要であることが示唆された。

A. 研究目的

α-DGは、骨格筋膜上のジストロフィン・糖蛋白質複合体の主要な構成成分であり、*O*-マンノース型糖鎖を介して細胞外のラミニン、アグリン、パールカン等と結合している。POMGnT1はマンノースにGlcNacを転移する酵素であり、*POMGnT1*遺伝子の異常により、先天性筋ジストロフィーの一つmuscle-eye-brain病(MEB)が発症する。MEBの分子病態を調べる目的で、我々はPOMGnT1変異マウスをgene targeting法を用いて作出し、その骨格筋とその再生能力、筋衛星細胞の増殖能、分化能を調べた。

B. 研究方法

HE染色、CK測定、EB投与

マウス骨格筋の凍結切片をHE染色した。血清CKはDRI-CHEM3500(FUJIFILM)を用いて計測した。骨格筋膜の損傷を調べるため、0.01%エバンスブルー/PBSをマウス腹腔内に体重1gあたり0.01ml投与し、24時間後骨格筋切片を蛍光顕微鏡で観察した。

α-DGの免疫染色

α-DGの糖鎖を認識する抗体VIA4-1 (upstate)を反応させた後、ヤギ抗マウスIgG-Alexa Fluor® 568 (Molecular Probes)とDAPI(核)で染色した。

筋衛星細胞の調製と培養

マウス骨格筋を、0.2% collagenase type Ⅱで消化し、得られた単核の細胞を抗体染色した。SM/C-2.6陽性、CD31陰性、CD45陰性、Sca-1陰性分画（筋衛星細胞）を、FACS Vantage SE (BD)を用いて回収した。細胞は37℃、CO_2湿潤下で、マトリゲル(BD)コートしたdish上で増殖培地（20%ウシ胎児血清/DMEM＋bFGF（2.5 ng/ml）＋HGF（25 ng/ml）＋heparin（5 μg/ml））で培養した。筋分化誘導には2%ウマ血清/DMEMを用いた。

レトロウイルス作成と細胞への感染

6 cmコラーゲンコートdish (IWAKI)にPlat-Eパッケージング細胞を2×10^6 cells/dish播種した。10%FBS/DMEMで16時間培養後、GFPレトロウイルスベクタープラスミド、又はPOMGnT1-GFPレトロウイルスベクタープラスミドをFuGene6

(Roche)を用いてトランスフェクションした。48時間培養後、上清を回収し、Amicon Ultra (Milipore)を用いてウイルスを濃縮した。マトリゲルコートした6 well dishに4×10^4 cells/wellの密度で細胞を播種し、翌日レトロウイルス溶液を100 μl添加した。数日後FACSを用いてGFP陽性細胞（感染細胞）を分取した。

MTT assay

マトリゲルコートした24 well plateに1×10^4 cells/wellの密度で細胞を播種後、24時間毎に各wellに0.5% MTT溶液を100 μlずつ添加し、4時間後、培地を取り除き、酸性イソプロパノールを1 ml添加、回収し、遠心後、上清のOD_{590}を測定した。

(倫理面への配慮)

マウスを用いた実験では実験計画書を神経研究所小型動物実験倫理問題検討委員会へ提出し、承認を得、同研究所の定める小型実験動物倫理指針に従って実験を行った。

C. 研究結果

1. *POMGnT1*$^{-/-}$ではα–DGの糖鎖修飾が異常であったが、組織切片上では骨格筋の筋変性·壊死は目立たなかった。筋壊死の指標である血中CK値及びエバンスブルーの筋線維内への取り込みは軽度上昇していた。

2. 野生型及び*POMGnT1*$^{-/-}$から筋衛星細胞分画をFACSで分取し、20%FCSと2.5 ng/ml bFGFを添加したDMEM培地で培養し、MTTアッセイを行なった結果、*POMGnT1*$^{-/-}$筋衛星細胞の増殖能の著明な低下が認められた。

3. 2%ウマ血清を含む培地で筋衛星細胞に分化を誘導したところ、野生型と*POMGnT1*$^{-/-}$の間には筋管形成能に有意差はなかった。

4. レトロウイルスによるPOMGnT1発現回復によりα–DGの糖鎖修飾は完全に回復したが、増殖能は回復しなかった。

D. 考察

POMGnT1$^{-/-}$では、α–DGとラミニンとの結合能が顕著に低下している事から、POMGnT1$^{-/-}$由来の筋衛星細胞の増殖能の低下はα–DG–ラミニンの結合能の低下によると考えられたが，POMGnT1発現回復により増殖能が回復しなかった。　その原因については今後検討が必要である。

E. 結論

POMGnT1$^{-/-}$ではα–DGの糖鎖修飾が異常であったが、組織切片上では骨格筋の筋変性·壊死は目立たなかった。*POMGnT1*$^{-/-}$筋衛星細胞では細胞増殖能が低下していた。レトロウイルスベクターでPOMGnT1発現を回復させても筋衛星細胞のin vitroでの増殖能が回復しなかったことから、α–DG–ラミニンの結合はnicheでの筋衛星細胞の維持に重要である可能性がある。

F. 健康危険情報

なし

G. 研究発表

1. 論文発表

（発表誌名巻号・頁・発行年等も記入）

Nishiyama A, Ampong BN, Ohshima S, Shin JH, Nakai H, Imamura M, Miyagoe-Suzuki Y, Okada T, Takeda S. (2008) Recombinant Adeno-associated Virus Type 8-Mediated Extensive Therapeutic Gene Delivery into Skeletal Muscle of alpha-Sarcoglycan-Deficient Mice. ***Hum Gene Ther.*** 19:719-30.

Tanihata J, Suzuki N, Miyagoe-Suzuki Y, Imaizumi K, Takeda S. (2008) Downstream utrophin enhancer is required for expression of utrophin in skeletal muscle. ***J Gene Med.*** 10:702-13.

Motohashi N, Uezumi A, Yada E, Fukada S, Fukushima K, Imaizumi K, Miyagoe-Suzuki Y, Takeda S (2008) Muscle CD31(-) CD45(-) side population cells promote muscle regeneration by stimulating proliferation and migration of myoblasts. ***Am J Pathol.*** 173:781-91.

Segawa M, Yamamoto Y, Yahagi H, Kanematsu M, Sato M, Ito T, Uezumi A, Hayashi S, Miyagoe-Suzuki Y, Takeda S, Tsujikawa K, Yamamoto H (2008) Suppression of macrophage functions impairs skeletal muscle regeneration with severe fibrosis. ***Exp. Cell Res.*** 2008 Aug 22. [Epub ahead of print]

Miyagoe-Suzuki Y, Masubuchi N, Miyamoto K, Wada MR, Yuasa S, Saito F, Matsumura K, Kanesaki H, Kudo A, Manya H, Endo T, Takeda S. (2009) Reduced proliferative activity of primary POMGnT1-null myoblasts in vitro. ***Mech Dev.*** 126, 107-116.

Kanagawa M, Nishimoto A, Chiyonobu T, Takeda S, Miyagoe-Suzuki Y, Wang F, Fujikake N, Taniguchi M, Lu Z, Tachikawa M, Nagai Y, Tashiro F, Miyazaki J, Tajima Y, Takeda S, Endo T, Kobayashi K, Campbell KP, Toda T.(2009) Residual laminin-binding activity and enhanced dystroglycan glycosylation by LARGE in novel model mice to dystroglycanopathy. ***Hum Mol Genet.*** 18(4):621-31.

Chang H, Yoshimoto M, Umeda K, Iwasa T, Mizuno Y, Fukada SI, Yamamoto H, Motohashi N, Suzuki YM, Takeda S, Heike T, Nakahata T. (2009) Generation of transplantable, functional satellite-like cells from mouse embryonic stem cells. ***FASEB J.*** 2009 Jan 23. [Epub ahead of print]

2. 学会発表

国際学会

Miyagoe-Suzuki Y, Masubuchi N, Miyamoto K, Wada RR, Endo T, Takeda S. Abnormal glycosylation of alpha-dystroglycan results in poor proliferation and limited migration of muscle satellite cells. **6th International Society for Stem Cell Research Annual Meeting 2008.** June 11-14, 2008. Philadelphia, USA

国内学会

1. 増渕　菜弥、宮本　香織、和田　倫子、花岡　和則、遠藤　玉夫、鈴木　友子、武田　伸一
α-ジストログリカンの 0-マンノース型糖鎖修飾は骨格筋幹細胞の増殖と移動に重要である
第6回幹細胞シンポジウム　平成２０年５月１６－１７日、学術総合センター

H. 知的財産権の出願・登録状況
（予定を含む。）

1. 特許取得

なし

2. 実用新案登録

なし

3. その他

なし

III. 研究成果の刊行に関する一覧表

研究成果の刊行に関する一覧表

書籍

著者氏名	論文タイトル名	書籍全体の編集者名	書 籍 名	出版社名	出版地	出版年	ページ
Kanagawa M, Toda T.	Fukutin and Fukuyama congenital muscular dystrophy.	Taniguchi. N, et.al. eds	Glycoscience Lab Manual	Elsevier Japan	Japan	2008	309-312
Miyagoe-Suzuki Y, Uezumi A & Shin'ichi Takeda	Side population (SP) cells and skeletal muscle differentiation	Tsuchida K& Takeda S	Recent Advances of Skeletal Muscle Differentiation	Research Signpost	Fort P.O., Trivandrum-695 023, Kerala, India	In press	
Ito N& Miyagoe-Suzuki Y	Neuronal NOS as a regulator of muscle mass	Ohira Y	Muscle Cell Physiology	Research Signpost	Fort P.O., Trivandrum-695 023, Kerala, India	In press	

雑誌

発表者氏名	論文タイトル名	発表誌名	巻号	ページ	出版年
Kumazawa R, Tomiyama H, Li Y, Imamichi Y, Funayama M, Yoshino H, Yokochi F, Fukusako T, Takehisa Y, Kashihara K, Kondo T, Elibol B, Bostantjopoulou S, Toda T, Takahashi H, Yoshii F, Mizuno Y, Hattori N.	Mutation analysis of the PINK1 gene in 391 patients with Parkinson disease.	Arch Neurol	65	802-808	2008
Mizuta I, Tsunoda T, Satake W, Nakabayashi Y, Watanabe M, Takeda A, Hasegawa K, Nakashima K, Yamamoto M, Hattori N, Murata M, Toda T.	Calbindin 1, fibroblast growth factor 20, and α-synuclein in sporadic Parkinson's disease.	Hum Genet	124	89-94	2008

Sato S, Omori Y, Katoh K, Kondo M, Kanagawa M, Miyata K, Funabiki K, Koyasu T, Kajimura N, Miyoshi T, Sawai H, Kobayashi K, Tani A, Toda T, Usukura J, Tano Y, Fujikado T, Furukawa T.	Pikachurin, a dystroglycan ligand, is essential for photoreceptor ribbon synapse formation.	Nature Neurosci	11	923-931	2008
Fujikake N, Nagai Y, Popiel HA, Okamoto Y, Yamaguchi M, Toda T.	Heat shock transcription factor 1-activating compounds suppress polyglutamine-induced neurodegeneration through induction of multiple molecular chaperones.	J Biol Chem	283	26188-26197	2008
Wakayama Y, Inoue M, Kojima H, Yamashita S, Shibuya S, Jimi T, Hara H, Matsuzaki Y, Oniki H, Kanagawa M, Kobayashi K, Toda T.	Reduced expression of sarcospan in muscles of Fukuyama congenital muscular dystrophy.	Histol Histopathol	23	1425-1438	2008
Tomiyama H, Mizuta I, Li Y, Funayama M, Yoshino H, Li L, Murata M, Yamamoto M, Kubo SI, Mizuno Y, Toda T, Hattori N.	LRRK2 P755L variant in sporadic Parkinson's disease.	J Hum Genet	53	1012-1015	2008
Popiel HA, Nagai Y, Fujikake N, Toda T.	Delivery of the aggregate inhibitor peptide QBP1 into the mouse brain using PTDs and its therapeutic effect on polyglutamine disease mice.	Neurosci Lett	449	87-92	2009
Kanagawa M, Nishimoto A, Chiyonobu T, Takeda S, Miyagoe-Suzuki Y, Wang F, Fujikake N, Taniguchi M, Lu Z, Tachikawa M, Nagai Y, Tashiro F, Miyazaki J, Tajima Y, Takeda S, Endo T, Kobayashi K, Campbell KP, Toda T.	Residual laminin-binding activity and enhanced dystroglycan glycosylation by LARGE in novel model mice to dystroglycanopathy.	Hum Mol Genet	18	621-631	2009

Okamoto Y, Nagai Y, Fujikake N, Popiel HA, Yoshioka T, Toda T, Inui T.	Surface plasmon resonance characterization of specific binding of polyglutamine aggregation inhibitors to the expanded polyglutamine stretch.	Biochem Biophys Res Commun	378	634-639	2009
Tomita K, Popiel HA, Nagai Y, Toda T, Yoshimitsu Y, Ohno H, Oishi S, Fujii N.	Structure-activity relationship study on polyglutamine binding peptide QBP1.	Bioorg Med Chem	17	1259-1263	2009
Mitsui J, Mizuta I, Toyoda A, Ashida R, Takahashi Y, Goto J, Fukuda Y, Date H, Iwata A, Yamamoto M, Hattori N, Murata M, Toda T, Tsuji S.	Mutations for Gaucher disease confer a high susceptibility to Parkinson disease.	Arch Neurol	in press		
Shikishima C, Hiraishi K, Yamagata S, Sugimoto Y, Takemura R, Ozaki K, Okada M, Toda T, Ando J.	Is g an entity? A Japanese twin study using syllogisms and intelligence tests.	Intelligence	in press		
Yanagisawa A, Bouchet C, Quijano-Roy S, Vuillaumier-Barrot S, Clarke N, Odent S, Rodriguez D, Romero NB, Osawa M, Endo T, Lia TA, Seta N, Guicheney P.	*POMT2* intragenic deletions and splicing abnormalities causing congenital muscular dystrophy with mental retardation.	Eur J Med Genet	in press		
Ohsawa Y, Okada T, Kuga A, Hayashi S, Murakami T, Tsuchida K, Noji S, Sunada Y.	Caveolin-3 regulates myostatin signaling.	Acta Myol.	27	19-24	2008
Nishiyama A, Ampong BN, Ohshima S, Shin JH, Nakai H, Imamura M, Miyagoe-Suzuki Y, Okada T, Takeda S.	Recombinant adeno-associated virus type 8-mediated extensive therapeutic gene delivery into skeletal muscle of alpha-sarcoglycan-deficient mice	Hum Gene Ther	19	719-730	2008
Tanihata J, Suzuki N, Miyagoe-Suzuki Y, Imaizumi K, Takeda S.	Downstream utrophin enhancer is required for expression of utrophin in skeletal muscle	J Gene Med	10	702-713	2008

Motohashi N, Uezumi A, Yada E, Fukada S, Fukushima K, Imaizumi K, Miyagoe-Suzuki Y, Takeda S	Muscle CD31(-) CD45(-) side population cells promote muscle regeneration by stimulating proliferation and migration of myoblasts	Am J Pathol	173	781-791	2008
Segawa M, Yamamoto Y, Yahagi H, Kanematsu M, Sato M, Ito T, Uezumi A, Hayashi S, Miyagoe-Suzuki Y, Takeda S, Tsujikawa K, Yamamoto H	Suppression of macrophage functions impairs skeletal muscle regeneration with severe fibrosis	Exp Cell Res	314	3232-3244	2008
Miyagoe-Suzuki Y, Masubuchi N, Miyamoto K, Wada MR, Yuasa S, Saito F, Matsumura K, Kanesaki H, Kudo A, Manya H, Endo T, Takeda S.	Reduced proliferative activity of primary POMGnT1-null myoblasts in vitro	Mech Dev	126	107-116	2009
Chang H, Yoshimoto M, Umeda K, Iwasa T, Mizuno Y, Fukada SI, Yamamoto H, Motohashi N, Suzuki YM, Takeda S, Heike T, Nakahata T.	Generation of transplantable, functional satellite-like cells from mouse embryonic stem cells	FASEB J	In press		
戸田達史	福山型筋ジストロフィー	ビジュアル疾患解説 眼で見る遺伝病とターナー症候群	2	6-7	2008
戸田達史	孤発性パーキンソン病のゲノムワイドスクリーニング	ゲノム医学	8	21-26	2008
小林千浩 戸田達史	認知と遺伝子	Cognition and Dementia	7	35-43	2008
谷口真理子 戸田達史	筋ジストロフィー	小児内科	40	1308-1314	2008
水田依久子 戸田達史	孤発性パーキンソン病のメカニズム	成人病と生活習慣病	38	887-892	2008
戸田達史	Alzheimer 病と遺伝	成人病と生活習慣病	38	1205-1210	2008
戸田達史	福山型筋ジストロフィーの発見とその類縁疾患における病態	蛋白質 核酸 酵素	53	1771-1780	2008
砂田芳秀	抗マイオスタチン療法	医学のあゆみ	226	402-407	2008

IV. 研究成果の刊行物・別刷

nature
neuroscience

VOLUME 11 NUMBER 8 AUGUST 2008
www.nature.com/natureneuroscience

Pikachurin at the ribbon synapse
Task difficulty modulates attentional effects in V1
Hypoxia causes axon guidance deficits

nature
neuroscience

Pikachurin, a dystroglycan ligand, is essential for photoreceptor ribbon synapse formation

Shigeru Sato[1–3], Yoshihiro Omori[1], Kimiko Katoh[1], Mineo Kondo[4], Motoi Kanagawa[5], Kentaro Miyata[4], Kazuo Funabiki[6], Toshiyuki Koyasu[4], Naoko Kajimura[7], Tomomitsu Miyoshi[8], Hajime Sawai[8], Kazuhiro Kobayashi[5], Akiko Tani[1], Tatsushi Toda[5], Jiro Usukura[9], Yasuo Tano[2], Takashi Fujikado[2,3] & Takahisa Furukawa[1]

Exquisitely precise synapse formation is crucial for the mammalian CNS to function correctly. Retinal photoreceptors transfer information to bipolar and horizontal cells at a specialized synapse, the ribbon synapse. We identified pikachurin, an extracellular matrix–like retinal protein, and observed that it localized to the synaptic cleft in the photoreceptor ribbon synapse. *Pikachurin* null-mutant mice showed improper apposition of the bipolar cell dendritic tips to the photoreceptor ribbon synapses, resulting in alterations in synaptic signal transmission and visual function. Pikachurin colocalized with both dystrophin and dystroglycan at the ribbon synapses. Furthermore, we observed direct biochemical interactions between pikachurin and dystroglycan. Together, our results identify pikachurin as a dystroglycan-interacting protein and demonstrate that it has an essential role in the precise interactions between the photoreceptor ribbon synapse and the bipolar dendrites. This may also advance our understanding of the molecular mechanisms underlying the retinal electrophysiological abnormalities observed in muscular dystrophy patients.

The establishment of precise synaptic connections between neurons in the developing and mature CNS is crucial for normal nervous system functions, including perception, memory and cognition. Thus, elucidating the mechanisms by which synapses develop and are modified is a central aim in neurobiology. Over the past few decades, a large number of protein components have been identified that are required for synapse morphogenesis and neurotransmitter release[1,2]. However, the molecules and mechanisms underlying specific synapse connections in the vertebrate CNS are still poorly understood.

The neural retina is developmentally a part of the CNS and is where the first stage of visual signal processing occurs. Visual information is transmitted from photoreceptor cells to the ganglion cells via bipolar interneurons. The photoreceptor axon terminal forms a specialized structure, the ribbon synapse, which specifically connects photoreceptor synaptic terminals with bipolar and horizontal cell terminals in the outer plexiform layer (OPL) of the retina. Although various presynaptic factors that are required for synaptic ribbon structure, such as CtBp2/RIBEYE, piccolo and bassoon, have been identified[3,4], the mechanism of ribbon synapse apposition specific to bipolar and horizontal terminals remains totally unknown.

Mutations in the dystrophin-glycoprotein complex (DGC) cause various forms of muscular dystrophy[5]. Dystroglycan, a central component of the DGC, functions as a cellular receptor that is expressed in a variety of tissues, including the CNS[6]. Dystroglycan precursor protein is cleaved into two subunits, α-dystroglycan and β-dystroglycan[7]. α-dystroglycan is a heavily glycosylated extracellular protein and has the potential to bind to several extracellular proteins containing the laminin-G domain, including laminin-α1, laminin-α2, agrin, perlecan and neurexins[8–11]. The DGC components are also expressed in the retina[12–15]. Altered electroretinograms (ERGs) are frequently found in individuals with Duchenne and Becker muscular dystrophy, indicating that the DGC is necessary for normal retinal physiology[16–18]. However, the functional role of DGC in the retina is elusive.

We isolated and characterized mouse pikachurin, a dystroglycan ligand in the retina. To the best of our knowledge, pikachurin is the first dystroglycan ligand to interact with the presynaptic dystroglycan. Our results demonstrate that pikachurin is critically involved in both the normal photoreceptor ribbon synapse formation and physiological functions of visual perception. This may also shed light on the molecular mechanisms underlying the retinal

---

[1]Department of Developmental Biology, Osaka Bioscience Institute, 6-2-4 Furuedai, Suita, Osaka, 565-0874, Japan. [2]Department of Ophthalmology, Osaka University Graduate School of Medicine, 2-2 Yamadaoka, Suita, Osaka, 565-0871, Japan. [3]Department of Visual Science, Osaka University Graduate School of Medicine, 2-2 Yamadaoka, Suita, Osaka, 565-0871, Japan. [4]Department of Ophthalmology, Nagoya University Graduate School of Medicine, 65 Tsuruma-cho, Showa-ku, Nagoya, 466-8550, Japan. [5]Division of Clinical Genetics, Department of Medical Genetics, Osaka University Graduate School of Medicine, 2-2 Yamadaoka, Suita, Osaka, 565-0871, Japan. [6]Department of Systems Biology, Osaka Bioscience Institute, 6-2-4 Furuedai, Suita, Osaka, 565-0874, Japan. [7]Research Center for Ultrahigh-Voltage Electron Microscopy, Osaka University, 7-1 Mihogaoka, Ibaraki, Osaka, 567-0047, Japan. [8]Department of Physiology, Osaka University Graduate School of Medicine, 2-2 Yamadaoka, Suita, Osaka, 565-0871, Japan. [9]Department of Materials Physics and Engineering, Nagoya University Graduate School of Engineering, 1-1 Furo-cho, Chikusa-ku, Nagoya, 464-8603, Japan. Correspondence should be addressed to T.F. (furukawa@obi.or.jp).

Received 1 May; accepted 12 June; published online 20 July 2008; doi:10.1038/nn.2160

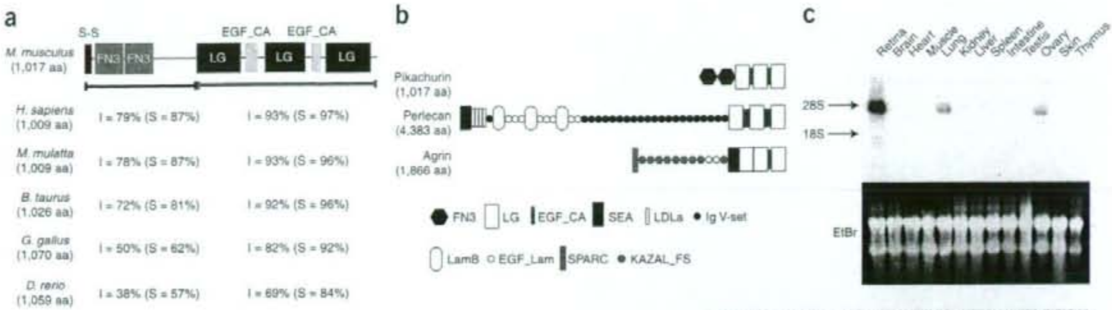

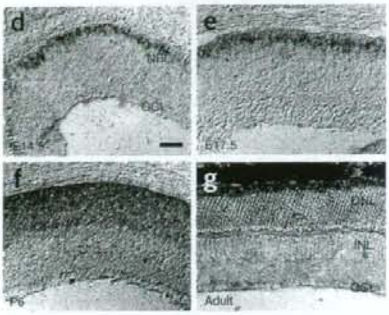

Figure 1 Molecular analysis and expression of *Pikachurin*. (**a**) Domain structure of mouse pikachurin. The percent amino acid identity (I) and similarity (S) between mouse and human, monkey, cow, chick or zebrafish in each of the amino-terminus portions and carboxyl-terminus portions are indicated. EGF_CA, calcium-binding EGF-like domain; LG, laminin G domain; S-S, signal sequence. (**b**) Schematic illustration of domain structures of mouse pikachurin, perlecan and agrin. The carboxyl end of pikachurin has substantial homology with that of agrin and perlecan. EGF Lam, laminin-type EGF-like domain; Ig V set, immunoglobulin V-set domain; KAZAL_FS, Kazal-type serine protease inhibitors and follistatin-like domain; LamB, laminin B domain; LDLa, low-density lipoprotein receptor domain class A; SEA, Domain found in sea urchin sperm protein, enterokinase and agrin; SPARC, secreted protein, acidic, and rich in cysteines domain. (**c**) Northern blot analysis of *Pikachurin* transcript in adult mouse tissues. The size of the pikachurin transcript is approximately 4.7 kb. Lower, ethidium bromide staining of RNA. Each lane contained approximately 10 μg of total RNA. (**d–g**) *In situ* hybridization analysis of mouse *Pikachurin* in the developing and adult retina. The *Pikachurin* signal was detected in the apical side of NBL at E14.5 (**d**) and E17.5 (**e**). P6 (**f**) and adult (**g**) retina had the *Pikachurin* signal in the prospective photoreceptor layer and the photoreceptor layer, respectively. GCL, ganglion cell layer; INL, inner nuclear layer; ONL, outer nuclear layer. Scale bar represents 50 μm.

electrophysiological abnormalities observed in individuals with Duchenne and Becker muscular dystrophy.

RESULTS

Isolation of pikachurin

Otx2 is an important transcription factor for the cell fate determination and development of retinal photoreceptor cells[19,20]. We previously reported that the cell fates of both rod and cone photoreceptors are converted to that of amacrine-like cells in the *Otx2* conditional knockout (CKO) mouse line that was created by mating *Otx2*$^{flox/flox}$ mice with *Crx-Cre* transgenic mice, which express cre recombinase in developing photoreceptors. We hypothesized that transcripts from various genes, which are important for photoreceptor development, maintenance and function, are relatively downregulated in the *Otx2* CKO retina compared with those of the wild-type retina. To identify genes that regulate photoreceptor development, we carried out a microarray analysis comparing the retinal gene expression profiles of wild-type and *Otx2* CKO mouse retinas (data not shown). In this screen, we identified *Pikachurin*, a gene that encoded a previously unknown extracellular matrix (ECM)-like protein containing laminin G and EGF-like domains (**Fig. 1a**).

To confirm whether or not *Pikachurin* transcription is regulated by Otx2, we carried out an RT-PCR analysis. *Pikachurin* expression was absent in the *Otx2* CKO mice retina (**Supplementary Fig. 1** online), indicating that *Pikachurin* is actually regulated by Otx2. We isolated a full-length cDNA and found that *Pikachurin* encodes a 1,017 amino acid protein that contains an N-terminal signal sequence, two fibronectin 3 (FN3), three laminin G and two EGF-like domains (**Fig. 1a** and **Supplementary Fig. 1**). We found that pikachurin was highly conserved in vertebrates, as indicated by the sequence similarity between mouse and zebrafish in the N-terminal FN3-containing domain (57%) and in the C-terminal laminin G repeats (84%) (**Fig. 1a** and **Supplementary Fig. 1**). The C-terminal half of pikachurin showed substantial similarity with agrin and perlecan (**Fig. 1b**).

Pikachurin is expressed in developing photoreceptors

To examine the tissue specificity of *Pikachurin* expression, we carried out a northern blot analysis with adult mouse tissues. We observed a single, strong 4.7-kb band in the mouse retina and faint bands in the lung and ovary (**Fig. 1c**). Although the *Pikachurin* transcript was not detected in the brain by northern blot analysis, we observed a faint *Pikachurin* band by RT-PCR analysis (**Supplementary Fig. 1**). We also detected *Pikachurin* expression in the pineal gland by RT-PCR but not in the inner ear at adult stage (**Supplementary Fig. 1**).

Furthermore, we carried out *in situ* hybridization using developing and adult mouse eye sections (**Fig. 1d–g**). *Pikachurin* expression was first detected at embryonic day 14.5 (E14.5) in the outer part of the neuroblastic layer (NBL), corresponding to the prospective photoreceptor layer (**Fig. 1d**). At this stage, cone genesis has reached its peak period and rod generation has been initiated[21]. At E17.5, a steady signal was observed (**Fig. 1e**). During postnatal retinal development, *Pikachurin* expression was observed in the photoreceptor layer (**Fig. 1f**) at postnatal day 6 (P6). This decrease in pikachurin expression in the later stages of photoreceptor development was confirmed by northern blotting (**Supplementary Fig. 1**). The expression level of pikachurin peaked at P6 and then decreased after this time point; however, a detectable level of pikachurin expression was maintained in the adult retina (**Fig. 1g**).

Pikachurin localizes in the vicinity of synaptic ribbon

To investigate the localization of pikachurin protein, we raised an antibody to pikachurin. We immunostained sections of adult mouse retina using this antibody. In the adult retina, pikachurin specifically localized to the OPL (**Fig. 2a**) in a punctate pattern (**Fig. 2b**). In

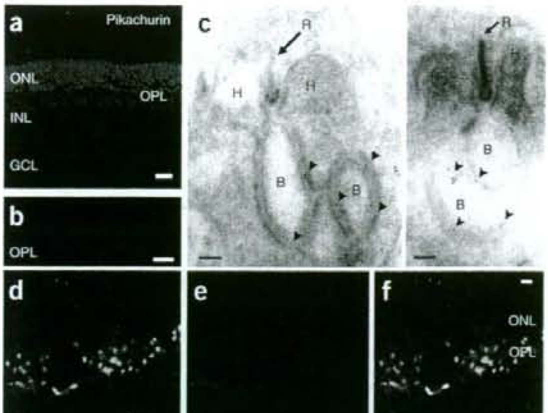

Figure 2 Pikachurin localizes to the synaptic cleft of photoreceptor ribbon synapse in the OPL. (**a**,**b**) Immunostaining of 6-month-old wild-type retina using antibody to pikachurin (red) with DAPI (blue) (**a**), which stains nuclei, or without DAPI at a higher magnification (**b**). Pikachurin localized to the OPL in the adult mouse retina in punctated pattern. Scale bars represent 20 μm in **a** and 10 μm in **b**. (**c**) Ultrastructural analysis of pikachurin localization in the ribbon synapse by electron microscopic immunocytochemistry. The pikachurin signals were localized to the synaptic cleft in the rod spherule (arrow heads). B and H indicate synaptic terminals of bipolar and horizontal cells, respectively. R indicates a synaptic ribbon. Scale bar represents 100 nm. (**d**–**f**) Confocal images of OPLs that were double-labeled with antibody to pikachurin (green) and PNA (red), a marker for cone pedicles of synaptic terminals, showing that pikachurin was colocalized with cone synaptic terminus. (**g**–**i**) Pikachurin-positive (green) puncta were localized to the INL side of horseshoe-like structures of synaptic ribbons that stained with CtBp2 (red), indicating that pikachurin is juxtaposed to, but not overlapping with, the synaptic ribbon structure. (**j**–**l**) Pikachurin (green) signal was observed at the photoreceptor side of mGluR6 staining (red), which is restricted to the postsynaptic site of the ON bipolar cells in the ribbon synapse of OPL. GCL, ganglion cell layer; INL, inner nuclear layer; ONL, outer nuclear layer; OPL, outer plexiform layer. Scale bars represent 20 μm in **d**–**l**.

contrast, no pikachurin signal was detected in the inner plexiform layer (IPL), where ribbon synapses are formed between bipolar cells and either ganglion or amacrine cells (data not shown).

To investigate more precisely the localization of pikachurin in the OPL, we carried out electron microscopic immunocytochemistry using our antibody to pikachurin. As shown in **Figure 2c**, the terminus of rod photoreceptors usually contains a single large ribbon that bends around four deeply invaginating postsynaptic elements, the dendrites of bipolar cells and processes of horizontal cells[3]. The pikachurin signals were mainly observed in the synaptic cleft around the bipolar cell dendritic tips in the rod spherule (**Fig. 2c**).

To examine whether pikachurin localizes to the cone pedicle, we immunostained the retina using our antibody to pikachurin and rhodamine-labeled peanut agglutinin (PNA), which specifically binds to glycolipids on the surface of cone pedicles[22]. PNA signals overlapped with those of pikachurin, indicating that pikachurin localized to cone synaptic terminals as well as to rod synaptic terminals (**Fig. 2d–f**).

Next, we analyzed the localization of pikachurin by staining with the synaptic ribbon markers bassoon and CtBp2/RIBEYE. Bassoon is a presynaptic cytomatrix protein that is essential for photoreceptor ribbon synapse formation and localizes to the base of the photoreceptor synaptic ribbon, a site of neurotransmitter release[23]. CtBp2/RIBEYE is a specific component of synaptic ribbons in the OPL and IPL of the retina[24]. We observed that pikachurin localized in the ribbon synapses to the inner nuclear–layer side of horseshoe-like structures of synaptic ribbons stained with bassoon (data not shown) and CtBp2/RIBEYE (**Fig. 2g–i**).

The localization of metabotropic glutamate receptor subtype 6 (mGluR6) is restricted to the postsynaptic site of ON bipolar cells in the ribbon synapses of the OPL[25]. We observed the pikachurin signal at the photoreceptor side of mGluR6 staining with a small partial overlap (**Fig. 2j–l**). These results suggest that pikachurin localizes to the synaptic cleft of the ribbon synapse primarily around the postsynaptic terminals of bipolar cells.

Pikachurin is required for apposition of bipolar dendrite

To investigate a possible role for *Pikachurin* in ribbon synapse formation and/or maintenance of the retina, we generated *Pikachurin* null mice by targeted gene disruption. We deleted the first exon, which contains a start codon, of the pikachurin open reading frame (**Fig. 3a**). We confirmed the deletion in the genomic DNA of the *Pikachurin* null mouse by Southern blot (**Fig. 3b**). Total RNAs from the adult retina were analyzed by northern blots using 5′ and 3′ fragments of mouse *Pikachurin* cDNA as probes. No substantial *Pikachurin* transcript or protein was detected in *Pikachurin* null mouse retinas (**Fig. 3c**,**d** and **Supplementary Fig. 2** online).

Pikachurin$^{-/-}$ mice were born in Mendelian ratios (data not shown). Both *Pikachurin*$^{+/-}$ and *Pikachurin*$^{-/-}$ mice showed no gross morphological abnormalities, and were viable and fertile under normal conditions in the animal facility. Histological examination revealed no obvious differences among wild-type, *Pikachurin*$^{+/-}$ and *Pikachurin*$^{-/-}$ mouse retinas at 6 months (**Fig. 3e–m** and **Supplementary Fig. 3** online).

To examine ultrastructural differences between wild-type and *Pikachurin*$^{-/-}$ mouse retinas, we carried out a conventional electron microscopy analysis. Although we did not find any substantial difference in the photoreceptor outer segments and ribbon synapses in the IPL (data not shown), we observed an absence of the tips of the bipolar cell dendrites in the *Pikachurin*$^{-/-}$ rod ribbon synapses (**Fig. 4a–d**) as well as those of cone photoreceptors (**Supplementary Fig. 4** online). To further examine this result, we analyzed the photoreceptor synaptic terminals of the wild-type and *Pikachurin*$^{-/-}$ retinas quantitatively (**Fig. 4e**). We prepared ultrathin sections from adult (3 month old) wild-type and *Pikachurin*$^{-/-}$ mouse retinas and randomly photographed them. For the quantitative analysis, we focused on rod photoreceptors, as they comprise ~99% of the photoreceptors in the

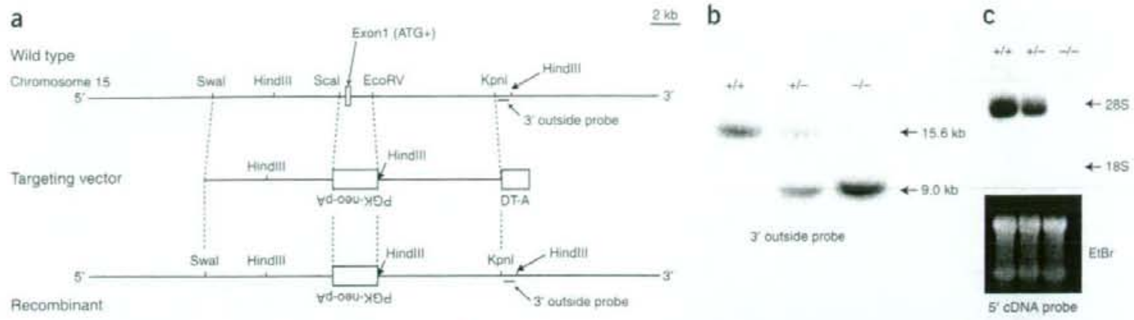

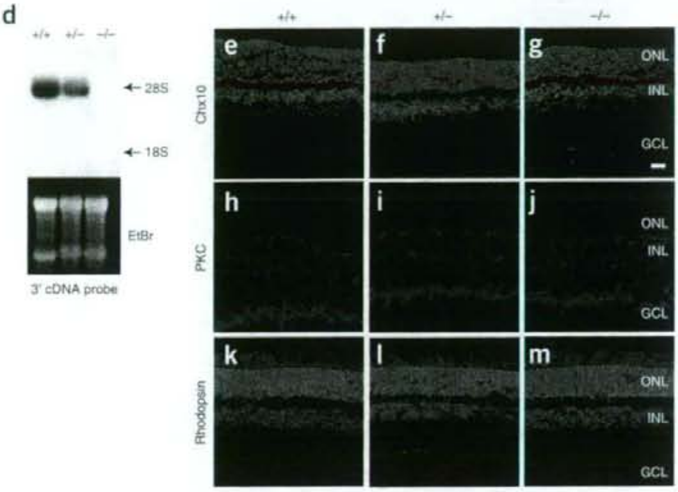

Figure 3 Generation of *Pikachurin* null mouse by targeted gene disruption. (**a**) Strategy for the targeted deletion of *Pikachurin* gene. Exon 1, which includes a start codon, was replaced with the PGK-neo cassette. The probe used for Southern blot analysis is shown (3' outside probe). (**b**) Southern blot analysis of genomic structure of *Pikachurin* locus to confirm the deletion of *Pikachurin* exon 1. *Hin*dIII-digested genomic DNA was hybridized with 3' outside probe. The probe detected 15.6-kb wild-type and 9.0-kb mutant bands. (**c**,**d**) Northern blot analysis of total RNA extracted from the retina derived from wild-type, *Pikachurin*$^{+/-}$ and *Pikachurin*$^{-/-}$ mice using 5' cDNA probe (**c**) and 3' cDNA probe (**d**) to confirm the lack of *Pikachurin* expression in the mutant mouse retina. (**e**–**m**) Immunostaining of wild-type and *Pikachurin* mutant retinal sections at 6 months of age. Immunohistochemical analysis using antibodies to Chx10 (bipolar cell nuclei marker, red, **e**–**g**), PKC (bipolar cell cytoplasmic marker, red, **h**–**j**) and rhodopsin (red, **k**–**m**) showed no obvious difference among wild-type, *Pikachurin*$^{+/-}$ and *Pikachurin*$^{-/-}$ mice retinas. Nuclei were stained with DAPI (blue). Scale bar represents 20 μm.

mouse retina[23]. A normal rod synaptic terminus contains a single ribbon synaptic site, where glutamate is released onto the postsynaptic elements, horizontal cell processes and rod bipolar cell dendrites. The postsynaptic elements invaginate into the rod terminal and form a triadic or tetradic configuration adjacent to the ribbon site (**Fig. 4a** and **Supplementary Fig. 5** online)[23,26]. In the adult *Pikachurin*$^{-/-}$ retina, we observed rod terminals containing invaginated bipolar terminals in only 3% of the sections, whereas we detected bipolar terminals in 53% of the wild-type retina (χ^2 test; $P < 0.001$; **Fig. 4e**). We used ultrathin sections; the vertical alignment of the sections was confirmed using photoreceptor outer segments as markers (**Fig. 4c,d**). We also found that the morphology of rod synaptic terminals varied widely even in the wild-type retina. Therefore, to confirm the precise structure of abnormal ribbon synapses in the adult *Pikachurin*$^{-/-}$ retina, we carried out electron tomography by ultrahigh-voltage electron microscopy (**Fig. 4f–k** and **Supplementary Movies 1–6**). We collected images from −60° to +60° at 2° intervals around a single axis from adult (3 month old) wild-type and *Pikachurin*$^{-/-}$ mouse retinas. The electron tomography indicates that in the terminals of bipolar cells do not appose to the synaptic terminals in the rod photoreceptor ribbon synapses the adult *Pikachurin*$^{-/-}$ retina (**Fig. 4j,k**).

We observed that the bipolar dendritic tips did not enter the invaginations in photoreceptor synaptic terminals in the *Pikachurin*$^{-/-}$ mice, but where do they end up? To address this question, we co-immunostained ribbon synapses using several synaptic markers. In the *Pikachurin*$^{-/-}$ mice, the bipolar cells, stained with protein kinase C (PKC; **Fig. 4l,m**), developed dendrites to the outer plexiform layer as well as they did in the wild type. mGluR6 accumulated at the tip of bipolar cell dendrites in both the wild-type and *Pikachurin*$^{-/-}$ mouse retina (**Fig. 4l,m**). CtBP2 was observed in the vicinity of the tips of bipolar dendrites in both the wild-type and *Pikachurin*$^{-/-}$ retina (**Fig. 4n,o**). A similar distribution of cone synaptic marker, PNA, was also observed in cone photoreceptor terminals (**Fig. 4p,q**). These data suggest that the bipolar dendritic terminals remain in close vicinity to photoreceptor terminals and seem to retain at least some integrity for the connection between photoreceptors and bipolar cells, even in the *Pikachurin*$^{-/-}$ retina.

Pikachurin is required for synaptic signal transmission

To evaluate the physiological function of *Pikachurin in vivo*, we measured ERGs on 2-month-old wild-type and *Pikachurin*$^{-/-}$ mice (**Fig. 5a–f**). The scotopic ERGs elicited by different stimulus intensities from a wild-type and a *Pikachurin*$^{-/-}$ mice are shown in **Figure 5a**. In the wild-type mouse, only a positive b-wave, which originates from the rod bipolar cells[27], was seen at lower stimulus intensities (−5.0 to −3.0 log cd s m^{-2}). At higher stimulus intensities (−1.0 to 1.0 log cd s m^{-2}), the negative a-wave, which originates mainly from the activity of the rod photoreceptors, appeared. The amplitude and implicit time of the a-wave of the dark-adapted ERGs were nearly the same for both types of mice, indicating that the rod photoreceptors are functioning normally in *Pikachurin*$^{-/-}$ mice (**Fig. 5a**). In contrast, the amplitude of the dark-adapted ERG b-wave in *Pikachurin*$^{-/-}$ mice

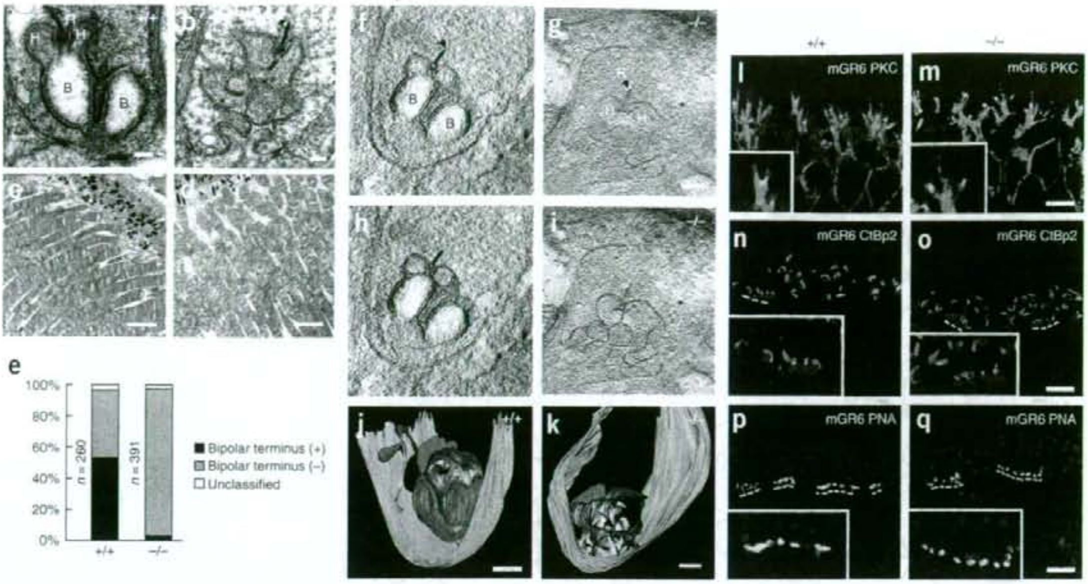

Figure 4 Pikachurin is required for proper apposition of bipolar dendritic tips to the photoreceptor synaptic terminus. (**a–d**) Ultrastructural analysis of ribbon synapses (**a**,**b**) and outer segments (**c**,**d**) in wild-type (**a**,**c**) and *Pikachurin*$^{-/-}$ (**b**,**d**) mouse retinas. Synaptic ribbon (R), horizontal cell processes (H) and bipolar cell dendrites (B) are shown. Scale bars represent 200 nm in **a** and **b** and 5 μm in **c** and **d**. (**e**) Quantitative analysis of defective bipolar cell dendrites in the wild-type (+/+) and *Pikachurin*$^{-/-}$ mouse retina. (**f–k**) Electron tomography of rod photoreceptor synapse terminals using ultrahigh-voltage electron microscopy. Representative images of retinal sections derived from wild-type (**f**,**h**,**j**) and *Pikachurin*$^{-/-}$ retinas (**g**,**i**,**k**). Representative demarcation of bipolar dendritic tips (magenta), horizontal processes (dark blue), ribbon (green) and rod plasma membrane (light blue) for tomography are shown for wild-type (**h**) and *Pikachurin*$^{-/-}$ (**i**) retinas (see **Supplementary Movies 1–6**). Scale bar = 300 nm. (**l–q**) Bipolar cell dendrites ended in the vicinity of photoreceptor terminals in *Pikachurin*$^{-/-}$ retina. mGluR6 (red) localized to the tip of bipolar cell dendrites stained with antibody to PKC (green) both in wild-type (**l**) and *Pikachurin*$^{-/-}$ retinas (**m**). The tips of bipolar cell dendrites stained with antibody to mGluR6 (red) localized in the vicinity of photoreceptor synaptic ribbons (green) both in the wild-type (**n**) and *Pikachurin*$^{-/-}$ retinas (**o**). Clustered cone synaptic terminals (broken lines) stained with PNA (green) colocalized with the tips of bipolar cell dendrites (red) in the wild-type (**p**) and the *Pikachurin*$^{-/-}$ (**q**) retinas.

was reduced at lower stimulus intensities of –5.0 to –3.0 log cd s m^{-2} but approached the normal range at higher stimulus intensities of –1.0 to 1.0 log cd s m^{-2} (**Fig. 5b**).

The most notable finding in this mutant mouse was the delay in the scotopic ERG b-wave (**Fig. 5c**). The implicit times of the scotopic ERG b-wave were severely delayed at all stimulus intensities, and the delay was more than 100 ms at the highest intensities. These results suggest that the signal transmission from the rod photoreceptors to the rod bipolar cells is less sensitive and is delayed in this mutant mouse.

To determine whether the abnormality in the signal transmission from the photoreceptors to the bipolar cells exists in the cone pathway, we recorded photopic ERGs from both types of mice (**Fig. 5d**). The amplitude of the a-wave of the photopic ERGs in *Pikachurin*$^{-/-}$ mouse was relatively larger than that of wild-type mouse, which was a result of the delay and reduction of the positive b-wave (**Fig. 5d**). The amplitude of the b-wave of the photopic ERGs was reduced and the implicit times were delayed at all stimulus intensities (**Fig. 5e,f**). These results indicate that the signal transmission from cone photoreceptors to the cone bipolar cells was also impaired in the *Pikachurin*$^{-/-}$ mouse.

We also recorded the collicular visual-evoked potentials (VEPs) in the *Pikachurin*$^{-/-}$ mouse. We did not observe any differences in the VEPs of wild-type and *Pikachurin*$^{-/-}$ mice in both scotopic and photopic conditions (**Fig. 5g,h**). This result suggests that VEPs may not be sensitive enough to reflect the ERG b-wave delay that we observed in the mutant retina and that the visual transmission pathway in the brain is not affected in *Pikachurin*$^{-/-}$ mice. We then investigated the optokinetic responses (OKRs) of 3-month-old wild-type and *Pikachurin*$^{-/-}$ mice induced by rotation of a screen with various spatial frequencies of black and white stripes (**Fig. 5i–k**). The *Pikachurin*$^{-/-}$ mouse showed similar OKRs by rotation of screens with 15- and 1.92-deg frequencies (gain was close to 1.0; **Fig. 5j,k**); however, its OKR at the 1.25-deg screen was significantly weaker than that of wild-type mice (unpaired *t* test, $P < 0.01$; **Fig. 5j,k**). Rotation of the 0.91-deg screen did not show significant OKR difference in either line ($P = 0.20$; **Fig. 5j,k**). Thus, *Pikachurin*$^{-/-}$ mice did not show noticeable impairment with relatively large angle stripes, but their sensitivity to small angle stripes was significantly impaired.

Pikachurin is a physiological ligand of α-dystroglycan

Many individuals with Duchenne muscular dystrophy (DMD) and Becker muscular dystrophy (BMD) have been known to show an abnormal dark-adapted ERG b-wave[17,28,29]. In mice, previous reports showed that certain dystrophin-disrupted alleles (*mdx*^{Cv2} and *mdx*^{Cv4}, alleles of *Dmd*) caused prolongation of the implicit time of the b-wave[18]. Functional defects of α-dystroglycan in *Large*-deficient mice (*Large*^{myd} and *Large*^{vls}) also produce a similar ERG phenotype to *Pikachurin* null mice[30]. In addition, agrin, perlecan and several laminin α-isoforms can all interact with α-dystroglycan by a laminin G domain–dependent mechanism[9]. These observations suggest that there is a possible functional interaction between dystroglycan and pikachurin. To investigate this issue, we first examined the localization of pikachurin, dystroglycan and dystrophin by co-immunostaining in the retina (**Fig. 6a–f**). At 6 months, pikachurin stained in a grainy pattern in the OPL of the retina (**Fig. 6a,d**). Notably, both β-dystroglycan and dystrophin were expressed in a similar grainy pattern, overlapping with pikachurin signals (**Fig. 6b,c,e,f**).

As shown above (**Fig. 1a,b**), structural anticipation suggests that pikachurin LG domains have similarity with LG domains of agrin and perlecan. Because both proteins are known to bind to α-dystroglycan via their LG domains[10,31], we investigated whether pikachurin LG domains bind to α-dystroglycan. To test this binding, we prepared recombinant pikachurin LG domains (residues 391–1,017) as a His-tag protein (pikachurin-LG–His) and recombinant α-dystroglycan as an Fc-fusion protein (DG-Fc). Pikachurin-LG–His was recovered in the NP-40–solubilized cell lysate. DG-Fc and its control Fc proteins were secreted into the cell culture media when expressed in NIH 3T3 cells. We confirmed that DG-Fc was recognized by a monoclonal antibody (IIH6) against glycosylated forms of α-dystroglycan (data not shown). We prepared DG-Fc–protein A beads, which were then mixed with the cell lysate that contained pikachurin-LG–His. The binding reaction was carried out in the presence of Ca^{2+} and Mg^{2+} or EDTA, as binding between α-dystroglycan and agrin or perlecan requires divalent cations[10,32,33]. Western blotting analysis of the bound materials using antibody to His revealed that the pikachurin LG domains bind to DG-Fc (**Fig. 6g**). This binding was inhibited by EDTA (**Fig. 6g**), which indicates that there is a divalent cation-dependent interaction, as is the case of laminin, agrin and perlecan[31]. We confirmed that pikachurin-LG–His did not bind to the Fc protein (**Fig. 6g**). In addition, the inhibitory effects of IIH6 (**Fig. 6h**) suggest that the pikachurin binding to α-dystroglycan is glycosylation-dependent, as IIH6 is reported to inhibit binding of laminin and perlecan[33,34]. Both

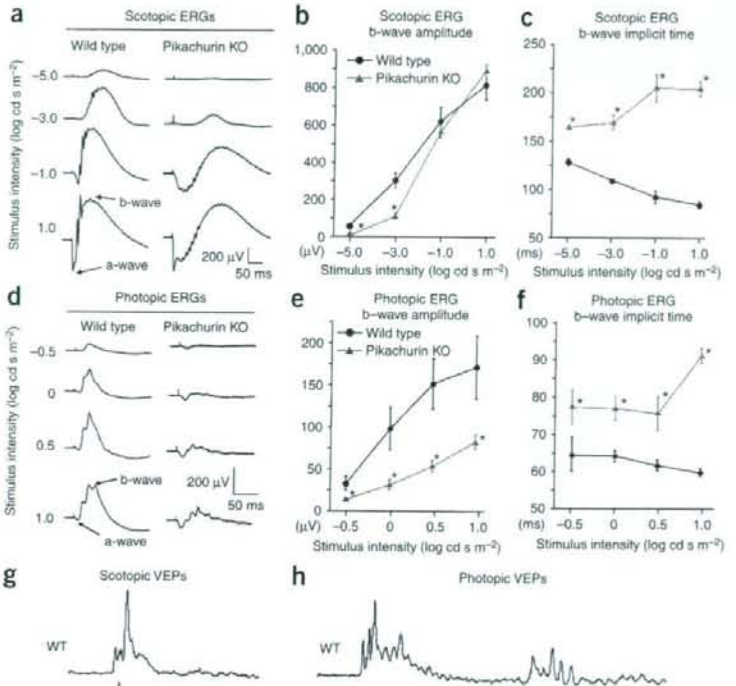

Figure 5 Electrophysiological and OKR analyses of wild-type and *Pikachurin* null mice. (**a–f**) ERG analysis of *Pikachurin*$^{-/-}$ mice. Scotopic (**a**) and photopic (**d**) ERGs were elicited by four different stimulus intensities from both wild-type and *Pikachurin*$^{-/-}$ (KO) mice ($n = 4$). Amplitude (**b**) and implicit time (**c**) of scotopic ERG b-waves as a function of the stimulus intensity are shown. Amplitude (**e**) and implicit time (**f**) of photopic ERG b-waves are shown. The bars indicate s.e.m. Asterisks indicate that the differences are statistically significant (Mann-Whitney test, $P < 0.05$). (**g,h**) VEPs in the superior colliculus of wild-type (WT) and *Pikachurin*$^{-/-}$ (KO) mice. (**g**) Under scotopic conditions, a brief 10-ms stimulation was applied from the LED panel (238 cd m^{-2}) in the front of the left eye. (**h**) Under photopic condition, a 500-ms stimulation was applied to examine both ON and OFF responses. The bottom trace indicates the onset and offset of a light stimulus. Scale bar indicates 200 µV. (**i–k**) OKR analysis of wild-type and *Pikachurin*$^{-/-}$ mice. A schematic drawing of OKR recording (**i**). (**j**) Screen velocity, scale bar represents $10° s^{-1}$. Examples of OKRs in wild-type (black) and *Pikachurin*$^{-/-}$ (gray) mice with a 1.92-, 1.25- or 0.91-deg screen. (**k**) OKR gain with four screens of different stripe width. Bar indicates s.d. (gray triangle, *Pikachurin*$^{-/-}$ mice; black circle, wild-type mice, $n = 6$). OKR of *Pikachurin*$^{-/-}$ mice with 1.25-deg screen was significantly weaker than that of wild-type mice (unpaired t test, $P < 0.01$).

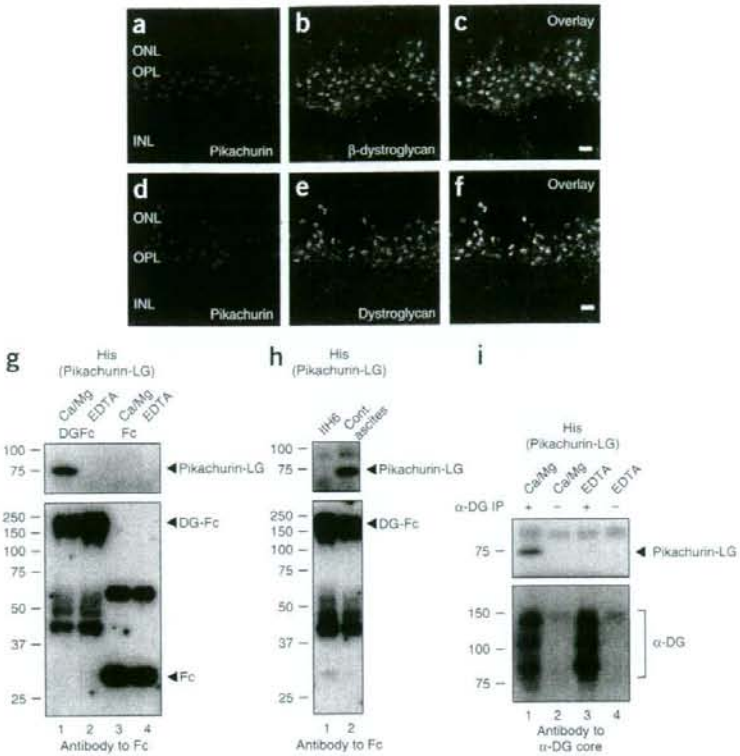

Figure 6 Interaction and colocalization of pikachurin with dystroglycan. (**a**–**f**) Confocal images of OPLs that were double labeled with antibodies to pikachurin (red, **a**,**d**) and β-dystroglycan (green, **b**) or dystrophin (green, **e**), showing that pikachurin colocalized with DGC molecules (**c**,**f**). Scale bars represent 2 μm. (**g**) Molecular interaction between pikachurin and α-dystroglycan. DG-Fc (lanes 1 and 2) or Fc (lanes 3 and 4) proteins were coupled with protein A beads and incubated with cell lysates containing pikachurin-LG–His in the presence of Ca^{2+} and Mg^{2+} (lanes 1 and 3) or EDTA (lanes 2 and 4). Bound materials were analyzed by western blotting with antibody to His tag (upper). A comparable amount of DG-Fc or Fc proteins on protein A beads were confirmed by staining with an antibody to Fc (lower). (**h**) Inhibitory effect of IIH6 on the interaction between pikachurin and α-dystroglycan. The binding reaction was carried out with (lane 1) or without (lane 2) the monoclonal antibody to α-dystroglycan IIH6. IIH6 selectively recognized glycosylated forms of α-dystroglycan. (**i**) Pikachurin interaction with eye α-dystroglycan. Native α-dystroglycan was immunoprecipitated from mouse eye extracts with antibody to α-DG core protein (lanes 1 and 3). For negative controls, antibody to α-DG core protein was omitted (lanes 2 and 4). The eye α-DG–protein G beads were tested for pikachurin binding in the presence of Ca^{2+} and Mg^{2+} (lanes 1 and 2) or EDTA (lanes 3 and 4). The samples were analyzed by western blotting with antibodies to His tag and α-DG core.

laminin and perlecan require α-dystroglycan glycosylation, which is recognized by IIH6, for binding to α-dystroglycan[35]. These data provide evidence of a direct interaction between pikachurin and α-dystroglycan.

To confirm the physiological interaction between pikachurin and α-dystroglycan in the retina, we carried out a pull-down assay using dystroglycan purified from murine retina. α-dystroglycan was immunoprecipitated from an eye extract using a specific antibody and assayed for an interaction with pikachurin. Consistent with our results using the recombinant α-dystroglycan, α-dystroglycan purified from murine eye interacts with pikachurin in a divalent cation–dependent manner (**Fig. 6i**). Furthermore, immunofluorescence analysis showed colocalization of pikachurin with both dystroglycan and dystrophin in the OPL (**Fig. 6a–f**), suggesting that pikachurin is a physiological ligand of α-dystroglycan in the retina.

DISCUSSION

Functional roles of *Pikachurin* in ribbon synapse formation

Structurally, synapses are specialized sites of cell-cell contact. Cell adhesion molecules and ECM proteins have been suspected, and in some cases have been demonstrated, to be important in synapse development and plasticity. In *Drosophila*, N-cadherins on both photoreceptor cells and their target neurons in the optic neuropil are required for proper target selection[36]. In vertebrates, however, cadherins do not seem to function in target recognition[37]. Agrin, an ECM molecule, has been extensively studied and proven to be required for postsynaptic differentiation, especially clustering of acetylcholine receptors, of the neuromuscular junction (NMJ)[38]. However, the effect and function of these cell adhesion and ECM molecules in synapse formation in the vertebrate CNS remain poorly understood. In the current study, our results demonstrate that a previously unknown ECM-like protein, pikachurin, is essential for proper bipolar dendritic tip apposition to the photoreceptor ribbon synapse. Notably, in the *Pikachurin* null retina, the tips of the bipolar cell dendrites are absent in photoreceptor ribbon synapse, but the horizontal cell terminus is not substantially affected. Immunostaining with antibody to mGluR6 or PKC in *Pikachurin* null retina did not show substantial differences in bipolar morphology (**Fig. 4l,m**), suggesting that bipolar cell differentiation is not perturbed. ERG studies showed that synaptic signal transmission from photoreceptors to bipolars was substantially prolonged but not lost. This suggests that the tips of the bipolar cell dendrites do not enter the invagination of photoreceptor terminals but still exist some distance apart from the ribbon synapse. This phenotype may be due to supporting molecules involved in photoreceptor-bipolar interaction, although pikachurin has a major role. Does the absence of the bipolar cell dendrite tips in the photoreceptor synapse occur because of a developmental defect or a maintenance abnormality after a normal synapse develops? Dynamic *Pikachurin* expression in developing photoreceptors (**Fig. 1d–g** and **Supplementary Fig. 1**) suggests that this phenotype is the result of developmental defects.

In this study, we focused our analysis on rod photoreceptor synapses (**Fig. 4a–k**), as the very small number of cones makes analysis with enough numbers of samples extremely difficult. However, several micrographs of cone synaptic terminals (**Supplementary Fig. 4**) and ERG results (**Fig. 5d–f**) suggest that similar synaptic abnormality probably occurs in cone photoreceptor synapses as was observed in rods. Typical ribbon synapses also exist in bipolar cell terminals in retinal IPL and hair cells in the inner ear. Pikachurin expression was not detected in these sites, suggesting that pikachurin functions specifically in photoreceptor-bipolar synaptic apposition.

The human *PIKACHURIN* gene is located on chromosome 5, region p13.2-p13.1. Although human *PIKACHURIN* maps in the vicinity of early-onset autosomal dominant macular dystrophy (MCDR3), which was mapped to chromosome 5, region p13.1-p15.33 (RetNet, http://www.sph.uth.tmc.edu/Retnet/), *PIKACHURIN* mutations do not seem to be responsible for this disease when the phenotypes of the *Pikachurin* null mouse are taken into consideration. Notably, the *Pikachurin* null mouse showed an impairment of visual function detected by OKR (**Fig. 5i–k**). *Pikachurin* null mice showed normal visual function for large-angle stripes but significantly reduced visual function for small-angle stripes (unpaired *t* test, $P < 0.01$). This may suggest that a mutation of *PIKACHURIN* in humans leads not to an obvious clinical manifestation of eye disease but rather to impairment of spatial resolution in vision.

Functional interaction between pikachurin and dystroglycan

Our observations suggest the possibility of a functional interaction between pikachurin and dystroglycan (**Supplementary Fig. 6** online). We observed a reduction in the amplitude and delayed implicit time of the ERG b-wave (**Fig. 5a–f**) in the *Pikachurin*$^{-/-}$ mouse. Both in human and mouse, mutations of dystrophin, an intracellular component of the DGC, are known to cause an abnormality in the ERG b-wave. In humans, many individuals with DMD and BMD with mutations in dystrophin show abnormal dark-adapted ERG b-waves[17,28]. Studies of individuals with DMD deletions have shown that the location of the deleted sequence can affect the ERG phenotype[29]. Mutations in the central or 3′ region of the gene are associated with severe reductions of amplitude and prolongation of the implicit time in the b-wave, whereas mutations limited to the 5′ end of the gene appear to be associated with milder abnormalities and, in some cases, normal ERGs[29]. In mice, disruption of dystrophin (*mdx*^{Cv2} and *mdx*^{Cv4}) causes prolongation of the implicit time of the b-wave[18]. Our results suggest that functional disruption of the interaction between dystroglycan and pikachurin in the retina may produce abnormal dark-adapted ERG b-waves in individuals with DMD and BMD. In addition, lack of glycosylation of α-dystroglycan in glycosyltransferase-deficient mice (*Large*^{myd} and *Large*^{vls}) also shows an ERG phenotype that is similar to that of *Pikachurin* null mice[30]. The similarity of unique abnormalities of ERGs observed in the *Pikachurin* null, *mdx*^{Cv2}, *mdx*^{Cv4}, *Large*^{myd} and *Large*^{vls} mutants strongly suggest that there is a functional interaction between pikachurin and DGC components in the retinal ribbon synapses.

We also found a direct interaction of pikachurin with α-dystroglycan, an extracellular component of the DGC (**Fig. 6**). It has been reported that α-dystroglycan binds to laminins and perlecan in a glycosylation-dependent manner[35]. The inhibitory effect of IIH6 and divalent cation–dependent binding suggest that pikachurin binds to α-dystroglycan by a mechanism that is similar to other known ligands, such as laminins and perlecan. Supporting this idea, pikachurin colocalizes with β-dystroglycan in photoreceptor synaptic terminals (**Fig. 6a–c**).

On the basis of these data, pikachurin probably functionally interacts with DGC components to form proper synaptic connections between photoreceptors and bipolar cells in the retinal ribbon synapses.

Molecular mechanism of pikachurin in synapse formation

In NMJs, formation of the proper synaptic structure is regulated by several dystroglycan ligands, such as agrin, laminins and perlecan. These ligands interact with dystroglycan, localizing to the postsynaptic surface of NMJ, and induce the differentiation and maturation of postsynaptic structures through the clustering of appropriate postsynaptic components (**Supplementary Fig. 6**)[39,40]. In contrast to the postsynaptic localization of dystroglycan in NMJs, dystroglycan in the ribbon synapse localizes to the presynaptic membrane of photoreceptor synaptic terminals around the bipolar cell dendritic processes[12–14]. To the best of our knowledge, pikachurin is the first dystroglycan ligand that has been found to interact with the presynaptic dystroglycan (**Supplementary Fig. 6**). How does pikachurin control invagination by the bipolar dendritic tips of the photoreceptor presynaptic terminals? On the basis of our data and previous findings, we hypothesize two scenarios. The first scenario is that pikachurin is involved in forming the proper structure of photoreceptor terminals for invagination by the tips of bipolar dendrites. The interaction of pikachurin with dystroglycan on the surface of the presynapse may cause a structural change of the photoreceptor presynaptic terminals, forming the proper connection with the postsynaptic terminals of bipolar dendrites. This scenario leads to the hypothesis that fine structural conformation of the axon terminus is crucial for the initial specific and precise synaptic apposition of a dendrite to the axon terminus. After this, adhesive molecules function supportively for the successive development and maintenance of synaptic connections.

The second scenario is that pikachurin is an attractant that induces the bipolar dendritic tips into proximity with the photoreceptor ribbon synapse through interaction with an unknown factor (represented as a factor, X; **Supplementary Fig. 6**) on the postsynaptic terminals of bipolar cell dendrites. Pikachurin released from photoreceptor synapses may induce structural changes in bipolar dendritic tips, such as the clustering of postsynaptic components, via an interaction with the unknown factor expressed in the tips of the bipolar cell dendrites. This may result in the attraction and insertion of the bipolar dendritic tips to the invagination of photoreceptor synaptic terminals.

In this study, we demonstrated that a previously unknown dystroglycan-interacting protein, pikachurin, is important for the formation of the ribbon synapse, a specialized synaptic structure in the CNS. Dystroglycan is known to be expressed not only in muscular cells but also in various CNS neurons[41]. Our findings provide clues as to the mechanisms of dystroglycan and ECM molecules in the formation of fine CNS synaptic structures.

METHODS

Generation of *Pikachurin* mutant mouse. We obtained *Pikachurin* genomic clones from a screen of the 129/SvEv mouse genomic DNA library (Stratagene). We subcloned an 8.4-kb *Swa*I-*Sca*I fragment and an 8.1-kb *Eco*RV-*Kpn*I fragment from the *Pikachurin* genomic clones into a modified pPNT vector[42], and transfected the linearized targeting construct into TC1 embryonic stem cell line[42]. The culture, electroporation and selection of TC1 were carried out as previously described[42]. Embryonic stem cells that were heterozygous for the targeted gene disruption were microinjected into C57BL/6 blastocysts to obtain chimeric mice.

We carried out immunohistochemistry, northern blot analysis, RT-PCR analysis, *in situ* hybridization, electron microscopy, ERG recordings, VEP recording, OKR analysis and pull down binding assays as described in the **Supplementary Methods** online.

Note: Supplementary information is available on the Nature Neuroscience website.

ACKNOWLEDGMENTS

We thank Y. Kambara, M. Murai, T. Tsujii, E. Oiki, S. Takiuchi and K. Sone for technical assistance; Y. Saijoh, M. Uehara and H. Hamada for advice on the production of a knockout mouse; and N. Maeda for statistical analysis. This work was supported by Molecular Brain Science, Grant-in-Aid for Scientific

Research on Priority Areas and Grant-in-Aid for Scientific Research (B), Grand-in-Aid for Exploratory Research, Specially Designated Research Promotion, Takeda Science Foundation, Senri Life Science Foundation, The Uehara Memorial Foundation and Mochida Memorial Foundation for Medical and Pharmaceutical Research. A part of this work was supported by the Nanotechnology Network Project of the Ministry of Education, Culture, Sports, Science and Technology Japan at the Research Center for Ultrahigh-Voltage Electron Microscopy, Osaka University (Handai Multi-functional Nano-Foundry).

AUTHOR CONTRIBUTIONS

S.S. and T. Furukawa designed the project. S.S., Y.O. and K. Katoh carried out the molecular, immunocytochemistry and electron microscopy experiments. S.S., M.K., K.M. and T.K. carried out the ERG experiments. S.S., A.T. and T. Furukawa produced the knockout mice. S.S. and N.K. performed the electron tomography analysis. J.U. carried out the immuno–electron microscopy experiments. S.S. and K.F. performed the OKR experiments. T.M. and H.S. carried out the VEP experiments. S.S., Y.O., M.K., K. Kobayashi and T.T. conducted the pull-down experiments. S.S., Y.O. and T. Furukawa wrote the manuscript. Y.T., T. Fujikado. and T. Furukawa supervised the project.

---

1. Waites, C.L., Craig, A.M. & Garner, C.C. Mechanisms of vertebrate synaptogenesis. *Annu. Rev. Neurosci.* **28**, 251–274 (2005).
2. Sudhof, T.C. The synaptic vesicle cycle. *Annu. Rev. Neurosci.* **27**, 509–547 (2004).
3. tom Dieck, S. & Brandstatter, J.H. Ribbon synapses of the retina. *Cell Tissue Res.* **326**, 339–346 (2006).
4. Sterling, P. & Matthews, G. Structure and function of ribbon synapses. *Trends Neurosci.* **28**, 20–29 (2005).
5. Straub, V. & Campbell, K.P. Muscular dystrophies and the dystrophin-glycoprotein complex. *Curr. Opin. Neurol.* **10**, 168–175 (1997).
6. Henry, M.D. & Campbell, K.P. Dystroglycan inside and out. *Curr. Opin. Cell Biol.* **11**, 602–607 (1999).
7. Ibraghimov-Beskrovnaya, O. *et al.* Primary structure of dystrophin-associated glycoproteins linking dystrophin to the extracellular matrix. *Nature* **355**, 696–702 (1992).
8. Sugiyama, J., Bowen, D.C. & Hall, Z.W. Dystroglycan binds nerve and muscle agrin. *Neuron* **13**, 103–115 (1994).
9. Winder, S.J. The complexities of dystroglycan. *Trends Biochem. Sci.* **26**, 118–124 (2001).
10. Talts, J.F., Andac, Z., Gohring, W., Brancaccio, A. & Timpl, R. Binding of the G domains of laminin α1 and α2 chains and perlecan to heparin, sulfatides, α-dystroglycan and several extracellular matrix proteins. *EMBO J.* **18**, 863–870 (1999).
11. Sugita, S. *et al.* A stoichiometric complex of neurexins and dystroglycan in brain. *J. Cell Biol.* **154**, 435–445 (2001).
12. Ueda, H., Gohdo, T. & Ohno, S. β-dystroglycan localization in the photoreceptor and Muller cells in the rat retina revealed by immunoelectron microscopy. *J. Histochem. Cytochem.* **46**, 185–191 (1998).
13. Jastrow, H., Koulen, P., Altrock, W.D. & Kroger, S. Identification of a β-dystroglycan-immunoreactive subcompartment in photoreceptor terminals. *Invest. Ophthalmol. Vis. Sci.* **47**, 17–24 (2006).
14. Schmitz, F. & Drenckhahn, D. Localization of dystrophin and β-dystroglycan in bovine retinal photoreceptor processes extending into the postsynaptic dendritic complex. *Histochem. Cell Biol.* **108**, 249–255 (1997).
15. Dalloz, C. *et al.* Differential distribution of the members of the dystrophin glycoprotein complex in mouse retina: effect of the *mdx(3Cv)* mutation. *Mol. Cell. Neurosci.* **17**, 908–920 (2001).
16. Cibis, G.W., Fitzgerald, K.M., Harris, D.J., Rothberg, P.G. & Rupani, M. The effects of dystrophin gene mutations on the ERG in mice and humans. *Invest. Ophthalmol. Vis. Sci.* **34**, 3646–3652 (1993).
17. Fitzgerald, K.M., Cibis, G.W., Giambrone, S.A. & Harris, D.J. Retinal signal transmission in Duchenne muscular dystrophy: evidence for dysfunction in the photoreceptor/depolarizing bipolar cell pathway. *J. Clin. Invest.* **93**, 2425–2430 (1994).
18. Pillers, D.A. Dystrophin and the retina. *Mol. Genet. Metab.* **68**, 304–309 (1999).
19. Nishida, A. *et al. Otx2* homeobox gene controls retinal photoreceptor cell fate and pineal gland development. *Nat. Neurosci.* **6**, 1255–1263 (2003).
20. Koike, C. *et al.* Functional roles of Otx2 transcription factor in postnatal mouse retinal development. *Mol. Cell Biol.* **27**, 8318–8329 (2007).
21. Carter-Dawson, L.D. & LaVail, M.M. Rods and cones in the mouse retina. I. Structural analysis using light and electron microscopy. *J. Comp. Neurol.* **188**, 245–262 (1979).
22. Iwasaki, M., Myers, K.M., Rayborn, M.E. & Hollyfield, J.G. Interphotoreceptor matrix in the human retina: cone-like domains surround a small population of rod photoreceptors. *J. Comp. Neurol.* **319**, 277–284 (1992).
23. Dick, O. *et al.* The presynaptic active zone protein bassoon is essential for photoreceptor ribbon synapse formation in the retina. *Neuron* **37**, 775–786 (2003).
24. Schmitz, F., Konigstorfer, A. & Sudhof, T.C. RIBEYE, a component of synaptic ribbons: a protein's journey through evolution provides insight into synaptic ribbon function. *Neuron* **28**, 857–872 (2000).
25. Nomura, A. *et al.* Developmentally regulated postsynaptic localization of a metabotropic glutamate receptor in rat rod bipolar cells. *Cell* **77**, 361–369 (1994).
26. Rao-Mirotznik, R., Harkins, A.B., Buchsbaum, G. & Sterling, P. Mammalian rod terminal: architecture of a binary synapse. *Neuron* **14**, 561–569 (1995).
27. Robson, J.G. & Frishman, L.J. Response linearity and kinetics of the cat retina: the bipolar cell component of the dark-adapted electroretinogram. *Vis. Neurosci.* **12**, 837–850 (1995).
28. Pillers, D.A. *et al.* Dystrophin expression in the human retina is required for normal function as defined by electroretinography. *Nat. Genet.* **4**, 82–86 (1993).
29. Sigesmund, D.A. *et al.* Characterization of the ocular phenotype of Duchenne and Becker muscular dystrophy. *Ophthalmology* **101**, 856–865 (1994).
30. Holzfeind, P.J. *et al.* Skeletal, cardiac and tongue muscle pathology, defective retinal transmission, and neuronal migration defects in the *Large* (*myd*) mouse defines a natural model for glycosylation-deficient muscle-eye-brain disorders. *Hum. Mol. Genet.* **11**, 2673–2687 (2002).
31. Hohenester, E., Tisi, D., Talts, J.F. & Timpl, R. The crystal structure of a laminin G–like module reveals the molecular basis of α-dystroglycan binding to laminins, perlecan and agrin. *Mol. Cell* **4**, 783–792 (1999).
32. Bowe, M.A., Deyst, K.A., Leszyk, J.D. & Fallon, J.R. Identification and purification of an agrin receptor from Torpedo postsynaptic membranes: a heteromeric complex related to the dystroglycans. *Neuron* **12**, 1173–1180 (1994).
33. Ervasti, J.M. & Campbell, K.P. A role for the dystrophin-glycoprotein complex as a transmembrane linker between laminin and actin. *J. Cell Biol.* **122**, 809–823 (1993).
34. Kanagawa, M. *et al.* Disruption of perlecan binding and matrix assembly by post-translational or genetic disruption of dystroglycan function. *FEBS Lett.* **579**, 4792–4796 (2005).
35. Michele, D.E. *et al.* Post-translational disruption of dystroglycan-ligand interactions in congenital muscular dystrophies. *Nature* **418**, 417–422 (2002).
36. Prakash, S., Caldwell, J.C., Eberl, D.F. & Clandinin, T.R. *Drosophila* N-cadherin mediates an attractive interaction between photoreceptor axons and their targets. *Nat. Neurosci.* **8**, 443–450 (2005).
37. Bozdagi, O., Valcin, M., Poskanzer, K., Tanaka, H. & Benson, D.L. Temporally distinct demands for classic cadherins in synapse formation and maturation. *Mol. Cell. Neurosci.* **27**, 509–521 (2004).
38. Sanes, J.R. & Lichtman, J.W. Induction, assembly, maturation and maintenance of a postsynaptic apparatus. *Nat. Rev. Neurosci.* **2**, 791–805 (2001).
39. Gee, S.H., Montanaro, F., Lindenbaum, M.H. & Carbonetto, S. Dystroglycan-α, a dystrophin-associated glycoprotein, is a functional agrin receptor. *Cell* **77**, 675–686 (1994).
40. Ervasti, J.M. & Campbell, K.P. Membrane organization of the dystrophin-glycoprotein complex. *Cell* **66**, 1121–1131 (1991).
41. Zaccaria, M.L., Di Tommaso, F., Brancaccio, A., Paggi, P. & Petrucci, T.C. Dystroglycan distribution in adult mouse brain: a light and electron microscopy study. *Neuroscience* **104**, 311–324 (2001).
42. Deng, C., Wynshaw-Boris, A., Zhou, F., Kuo, A. & Leder, P. Fibroblast growth factor receptor 3 is a negative regulator of bone growth. *Cell* **84**, 911–921 (1996).